Annual Project Summary – Year 2

December 1, 2004

Determination of in-situ S wave attenuation in the sediments of the Mississippi embayment using existing boreholes and validation of refraction techniques for the determination of Q_s

External Grant Award Number: 03HQGR0036

Jose Pujol
Center for Earthquake Research and Information
Phone: (901) 678-4827 Fax: (901) 678-4734 Email: pujol@ceri.memphis.edu

Shahram Pezeshk
Department of Civil Engineering
Phone: (901) 678-4727 Fax: (901) 678-3026 Email: spezeshk@memphis.edu

Scott Stovall
Department of Civil Engineering
Phone: (901) 678-3288 Email: spstovll@memphis.edu

Jiandang Ge
Center for Earthquake Research and Information
Phone: (901) 678-4809 Fax: (901) 678-4734 Email: jge@memphis.edu

The University of Memphis, Memphis, TN 38152

Non-technical summary

Reliable determination of attenuation in the sedimentary deposits of the Mississippi embayment is critical for reliable hazard prediction. Because our current knowledge in this area is very limited, the goal of our research is a detailed analysis of attenuation using SH wave data collected in nine boreholes drilled in western Tennessee to depths of up to 60 m. In addition, because drilling and casing of boreholes is expensive, a second goal of our research is to establish whether refraction data, which are easy to collect, can be used to determine reliable estimates of attenuation. Preliminary analysis of the borehole data shows that Q_s ranges between about 20 and 40, which confirms our earlier conclusion that Q_s can be significantly larger than the value of 10 found by other researchers in California and elsewhere.

Background

As is well known (e.g. Field, 2000, and references therein), unconsolidated or poorly consolidated sediments amplify the ground motion caused by seismic waves significantly, thus increasing the damage they cause. This is one of the reasons why structures built in sedimentary basins are at a higher risk than those built on hard rock. On the other hand, seismic wave attenuation in sediments can be high, which would contribute to a decrease in ground motion amplitudes. Therefore, a reliable estimate of the seismic attenuation in this kind of environments is necessary for a realistic assessment of seismic hazard. This is particularly true for the New Madrid seismic zone, which is covered by the sediments of the Mississippi embayment, with a thickness of about 1 km near Memphis, Tennessee.

Attenuation is usually quantified in terms of the inverse of the quality factor Q, and because most of the damage to buildings and structures in an earthquake arises from horizontal forces, for seismic risk studies the quantity of interest is the Q for shear waves (Q_s). In addition, because the determination of attenuation is based on variations of seismic wave amplitudes and shapes, establishing reliable values of Q_s requires the use of data recorded in boreholes. However, a drawback of borehole attenuation studies is the cost of drilling and casing and for this reason the number of values of Q_s determined for near-surface materials is small. A review of results from California and Japan (see Pujol et al., 2002) shows that in most cases Q_s is around 10 for depths around 100 m. On the other hand, our own results from three boreholes in the vicinity of Memphis show values of Q_s between 18 and 44 for depths reaching up to 60 m. The difference between these numbers and those obtained by other researchers is significant, as can be seen from the spectral ground motion amplification for different values of Q_s. For example, for a 100 m deep low-velocity layer a Q_s of 10 will significantly reduce the amplification due to the presence of the layer, while a Q_s of 30 will not (Pujol et al., 2002).

Shear-wave seismic source and borehole instrument

The seismic source we use in the borehole experiments is a shear wave generator similar to that described by Liu et al. (1996, 1997). Basically, it consists of a compressed-air driven hammer that slides on low-friction tracks. The hammer impacts on two anvils located on both sides of the hammer. The two impacts correspond to the forward and retracting motions of the hammer. The weight of a truck on the source gives a good coupling to the ground. The source was built by personnel of the Department of Civil Engineering at The University of Memphis using blueprints provided by Dr. Liu. This source is very repeatable, although in a previous experiment (Pujol et al, 2002) we have observed an increase in amplitude for the higher frequencies as the depth increases. Because the experiment was conducted from the surface down and the source position was unchanged, the amplitude increase for the higher frequencies is probably the result of a source-ground coupling that kept improving as the experiment proceeded. To account for these (slight) source variations we use a "source monitor", which is a three-component geophone at a fixed position on the surface to record the waves generated each time that the source is activated.

In our earlier attenuation work (Pujol et al., 2002) we used a 10 Hz three-component commercial borehole instrument. With this equipment the lower limit of the frequency range for reliable values of Q was 10 Hz. We tried to lower this limit by using 4.5 Hz geophones, which we added to the commercial instrument. This required a considerable amount of work, which is described in the Year 1 report.

Method used to determine Q_s

The determination of attenuation is based on the standard assumption of exponential amplitude decay in the frequency domain. For the the case of borehole data and a seismic source close to the borehole the variation in wave amplitudes can be represented by the following relation:

$$A_z(f) = (G_o/G_z)\, e^{-\alpha f} A_o(f) \tag{1}$$

where $A_o(f)$ is the amplitude of a reference wavelet at depth z_o, $A_z(f)$ is amplitude of a wavelet at depth z, α is the attenuation coefficient, and G_o and G_z are frequency-independent geometric spreading factors for depths z_o and z. A number of factors that may affect wave amplitudes and shapes are discussed in Pujol et al. (2002). The data recorded with the source monitor described above is used to extract A_o.

When the medium is homogeneous α is given by

$$\alpha = \pi \delta z / Q v; \qquad \delta z = z - z_o \tag{2a, b}$$

where v is the velocity of wave propagation in the medium. If α is independent of frequency, then one way to estimate Q is to fix z, to divide (1) by A_o and then to take logarithms on both sides. This gives

$$\ln \frac{A_z(f)}{A_o(f)} = -\alpha(z) f + \ln \frac{G_o}{G_z} \tag{3}$$

which is the equation of a straight line in f. In this context α is a function of z, known as cumulative attenuation, and can be determined by fitting a least squares line to the observations. Once $\alpha(z)$ has been computed, Q as a function of depth can be estimated using (2a). However, as scatter in the data may preclude the determination of reliable values of Q, we fit a straight line to $\alpha(z)$ for a range of values of z. Let k be the slope of the best-fit line. Then, from (2a) we get

$$k = \frac{\pi}{vQ} \tag{4}$$

so that

$$Q = \frac{\pi}{vk} \tag{5}$$

and

$$\alpha = k \delta z \tag{6}$$

The Q determined using (5) is an average value, and if $\alpha(z)$ is an approximately piecewise linear function of z, there will be a pair of values k and Q for each segment. Together with Q_s we also compute its standard deviation σ_Q (Pujol et al., 2002).

This method is based on Hauge (1981) and is convenient because it is not necessary to know the true amplitudes of the waves. When the assumption that α is independent of f is not valid, an alternative method is to fix f and let z vary (Pujol and Smithson, 1991). In this case it is critical to account for the geometric spreading correctly.

Data and preliminary data analysis

We collected nine VSPs in western Tennessee (see Fig. 1). Originally we had planned to work on ten sites, but two of them were not available; one was filled up with sand and the other was paved over. The quality of the VSP data is variable in spite of extremely careful field work. We have not been able to control this aspect of the data acquisition and this has delayed our data analysis, as we have had to work harder to ensure that our results are reliable. Some of the data are affected by one of the following two problems or both. In both cases the problem is that the shape of the downgoing waves is considerably different from that of the monitor traces recorded at the surface and also have significantly larger durations. The other problem is that for some VSPs some of the waveforms are quite different from the rest. These problems are very puzzling, and may be related to the coupling of the borehole casing to the surrounding soil or to changes in the lithology as a function of depth. Another possibility, which we are investigating with synthetic seismograms, is that some of the waveform variation is due to attenuation. When the data are not affected by quality problems the data analysis is straightforward, but when the VSP traces are different from the monitor traces the reference trace in eqn. (1) has to be replaced by one representative VSP trace.

Figures 2-4 show the steps carried out to estimate Q for the Covington VSP recorded with a 10 Hz geophone. Fig. 2 shows the monitor and VSP traces (left) and the windowed monitor and shifted VSP traces (right). Note the considerable difference in the two sets of waveforms. Fig. 3 shows the spectra of the windowed traces (left) and the spectral ratio computed using one of the actual traces as the reference wavelet. Because some of the VSP data are quite different from the rest, they are removed from the analysis. We suspect that some of the observed differences are due to changes in the lithology, but to test this hypothesis we will generate synthetic VSP's which will be analyzed as the actual data (Pujol and Smithson, 1991). The slopes of the best-fit lines on Fig. 3 (right) give the $\alpha(z)$ in eqn. (3). These values of α are plotted in Fig. 4. The slope of the corresponding best-fit line gives the k used in eqn. (4), which is used with eqn. (5) to compute Q. For this borehole Q is equal to 17 ± 2. This value is similar to that obtained by Pujol et al. (2002) for Marked Tree (18 ± 4).

Figures 5-7 show the data and results for the Covington borehole recorded with a 4.5 Hz geophones. We had expected that with this type of geophone we would be able to estimate values of Q for lower values of frequency, but unfortunately this has not been the case. The curvature of the spectral ratios for frequencies below about 10 Hz is present in all the datasets, and limits our ability to estimate Q for frequencies below this limit. For the frequencies above this limit the value of Q is equal to that computed using the 10 Hz data.

Figures 8-19 show the data and results for other VSP's. The largest values of Q are equal to 44 and 43 for two of the VSPs, which are surprisingly close to the value of 44 obtained for another VSP by Pujol et al. (2002).

We must note however, that the results presented in this report are preliminary, and that the we are carrying out additional work to assure that the most reliable values of Q have been determined. To achieve this goal we are using synthetic seismograms with three goals. (a) To improve the velocity estimates by matching the first few milliseconds of the downgoing waves. The first arrival times are usually difficult to determine, and for this reason some dominant feature is chosen to determine velocities, but because of the observed changes in waveforms, this approach introduces some errors. (b) To investigate the effect of variations in velocity and lithology on the computation of Q_s. Lithology logs are available. (c) To place constraints on the value of Q_s by waveform matching. The synthetic seismogram software (Wu, 1983) allows for attenuation (including dispersion) and for arbitrary input wavelets, and this versatility will be used to try to match the observed waveforms.

As noted above, borehole attenuation studies are not common because of high drilling and casing costs, and for these reason there have been attempts to determine Q_s using shallow SH wave refraction data (e.g., Wang et al., 1994). It is not clear, however, whether the values thus obtained really measure Q_s, and for this reason we are collecting SH wave refraction data at each borehole site for attenuation analysis. In this way it will be possible to establish whether the refraction data can be used instead of borehole data to estimate Q_s. The source for the refraction data is a sledgehammer impacting on an I-beam. For each borehole five source locations are used, with five unstacked shots per location. Figures 20-21 and 22-23 show representative traces collected in Brownsville and Jackson. Visual inspection of the data shows that there are considerable differences between the two data sets, with the shallow velocities significantly higher in the vicinity of the Jackson borehole.

Data availability

The borehole data and refraction data are available from S. Pezeshk (phone: 901-678-4727; email: spezeshk@memphis.edu) and J. Pujol (phone: 901-678-4827; e-mail: pujol@ceri.memphis.edu), respectively.

References

Field, E., and the SCEC Phase III working group (2000). Accounting for site effects in probabilistic seismic hazard analyses of southern California: overview of the SCEC Phase III working group, *Bull. Seism. Soc. Am.* **90**, S1-S31.

Liu, H.-P., Y. Hu, J. Dorman, T.-S. Chang, and J.-M. Chiu (1997). Upper Mississippi embayment shallow seismic velocities measured in situ, *Eng. Geology* **46**, 313-330.

Liu, H.-P., R. Maier, and R. Warrick (1996). An improved air-powered impulsive shear-wave source, *Bull. Seism. Soc. Am.* **86**, 530-537.

Pujol, J., S. Pezeshk, Y. Zhang, and C. Zhao (2002). Unexpected values of Q_s in the unconsolidated sediments of the Mississippi embayment, *Bull. Seism. Soc. Am.* **92**, 1117-1128.

Pujol, J., and S. Smithson (1991). Seismic wave attenuation in volcanic rocks from VSP measurements, *Geophysics* **56**, 1441-1455.

Wu, R-C. (1983). Frequency domain computation of synthetic vertical seismic profiles, M.S. thesis, Texas A&M University.

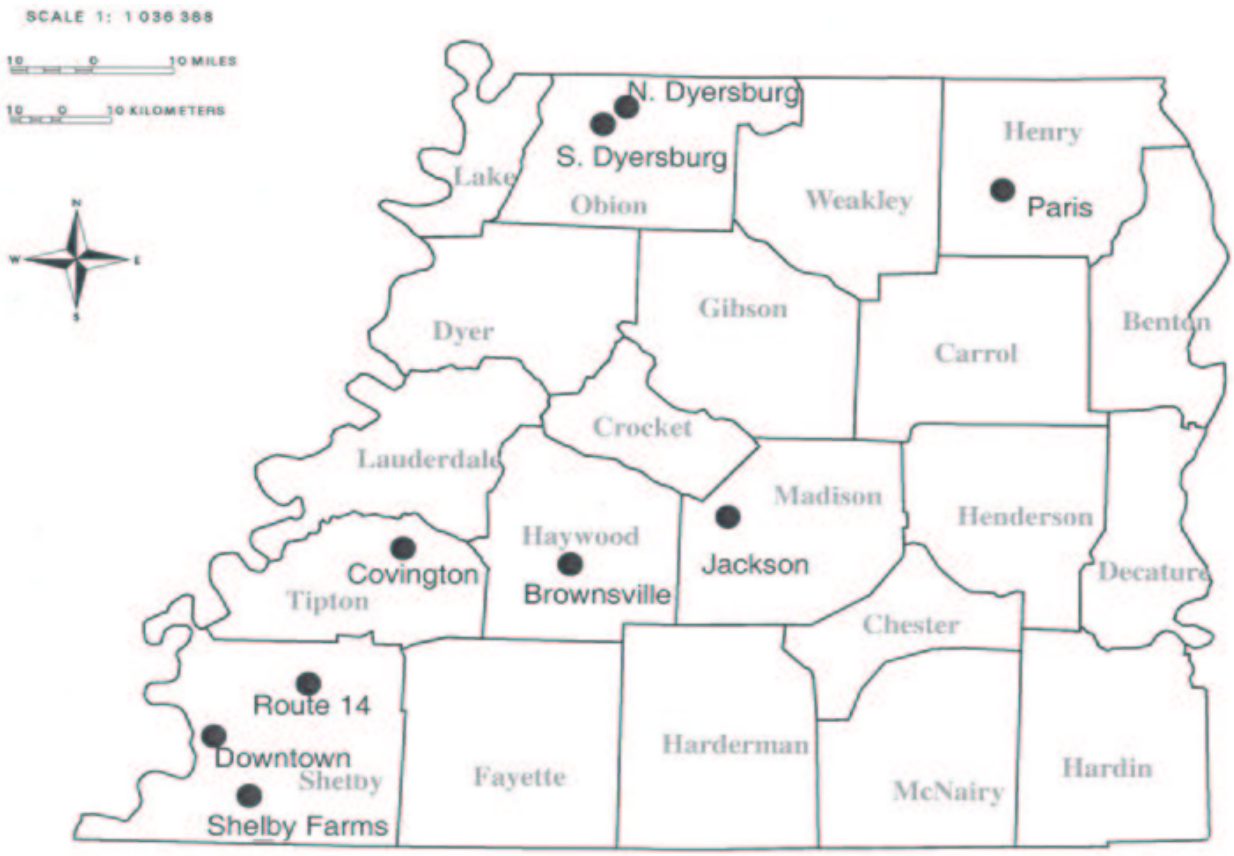

Figure 1: Map showing the sites in western Tennessee where VSP data have been collected (dots).

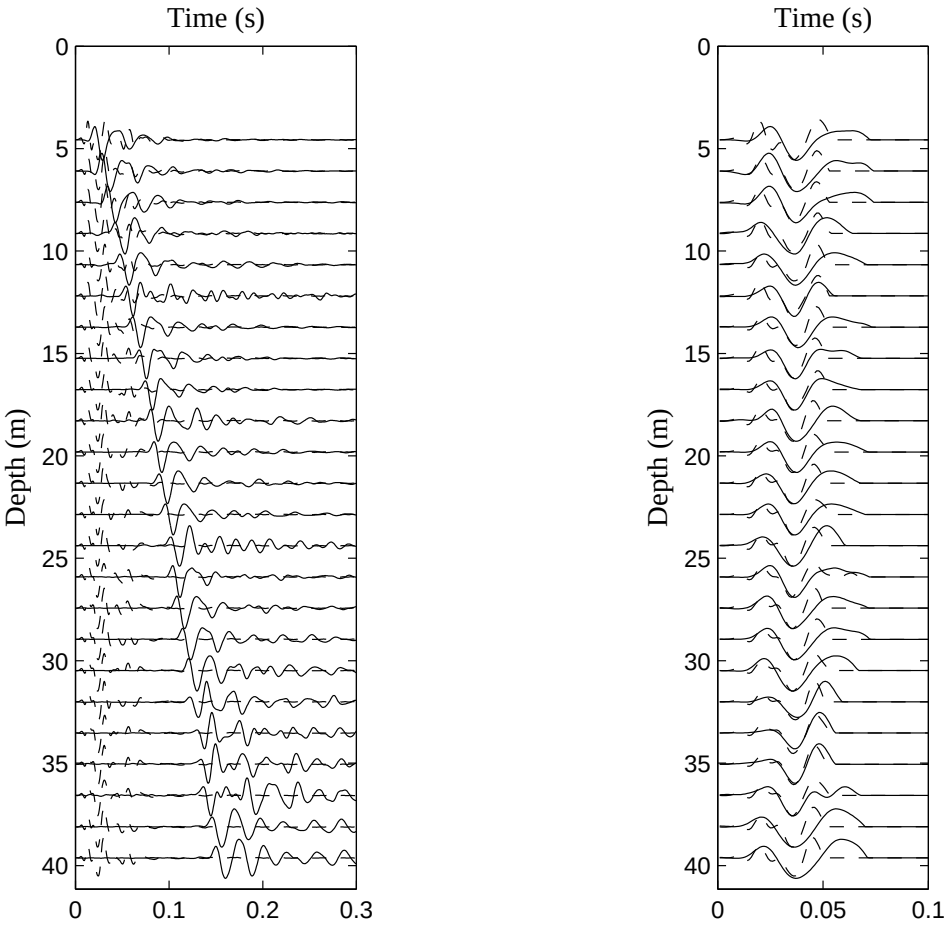

Figure 2: LEFT: Data recorded in the Covington borehole using a 10 Hz geophone (solid lines) and corresponding surface monitor traces (dashed lines). RIGHT: first cycles of the traces on the left used for the attenuation analysis.

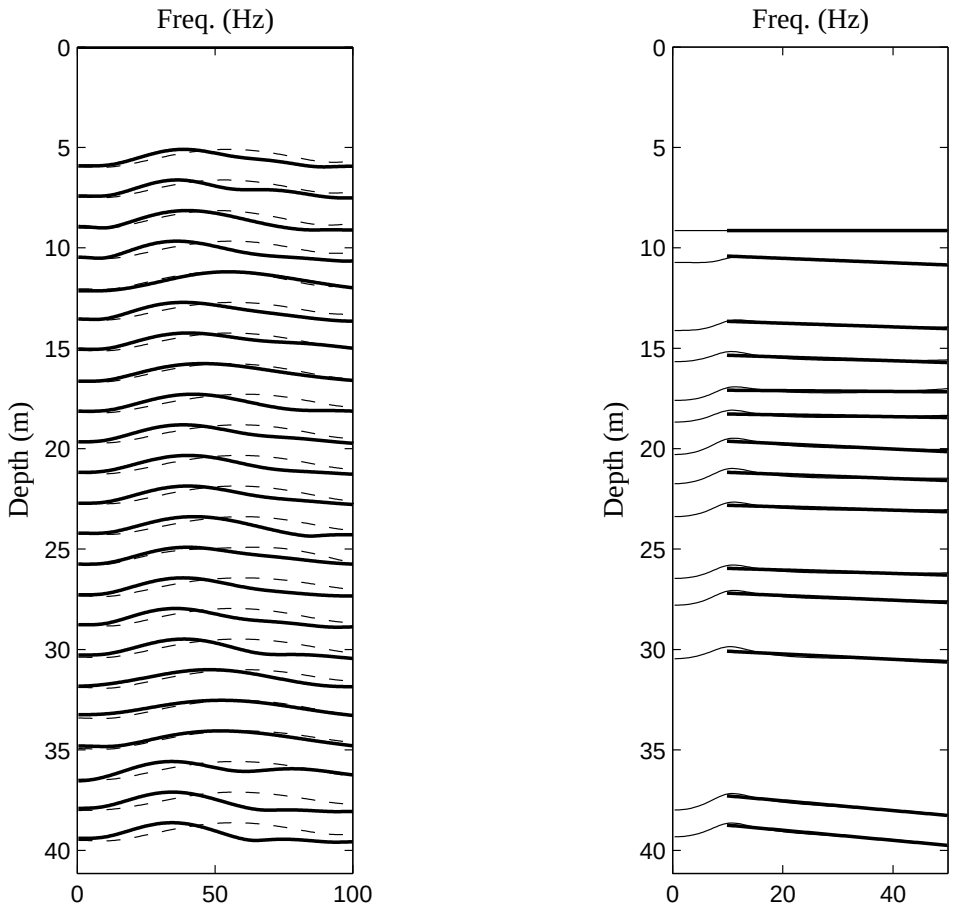

Figure 3: LEFT: Normalized spectra for the data on the right of Fig. 2. RIGHT: Spectral ratios for selected depths using the spectrum for the shallowest trace as reference (note that the ratio is a straight line). The bold line is the least-squares best fit line used to compute $\alpha(z)$ (see eqn. (3)).

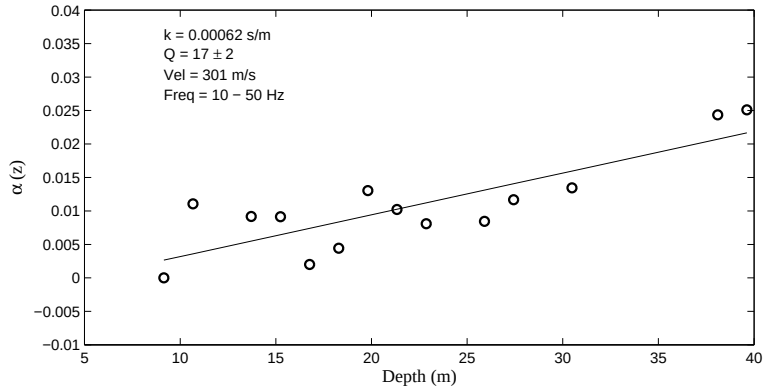

Figure 4: Attenuation curve for the Covington data for the 10 Hz geophone. Circles represent the cumulative attenuation α derived from Fig. 3. The best-fit line is also shown.

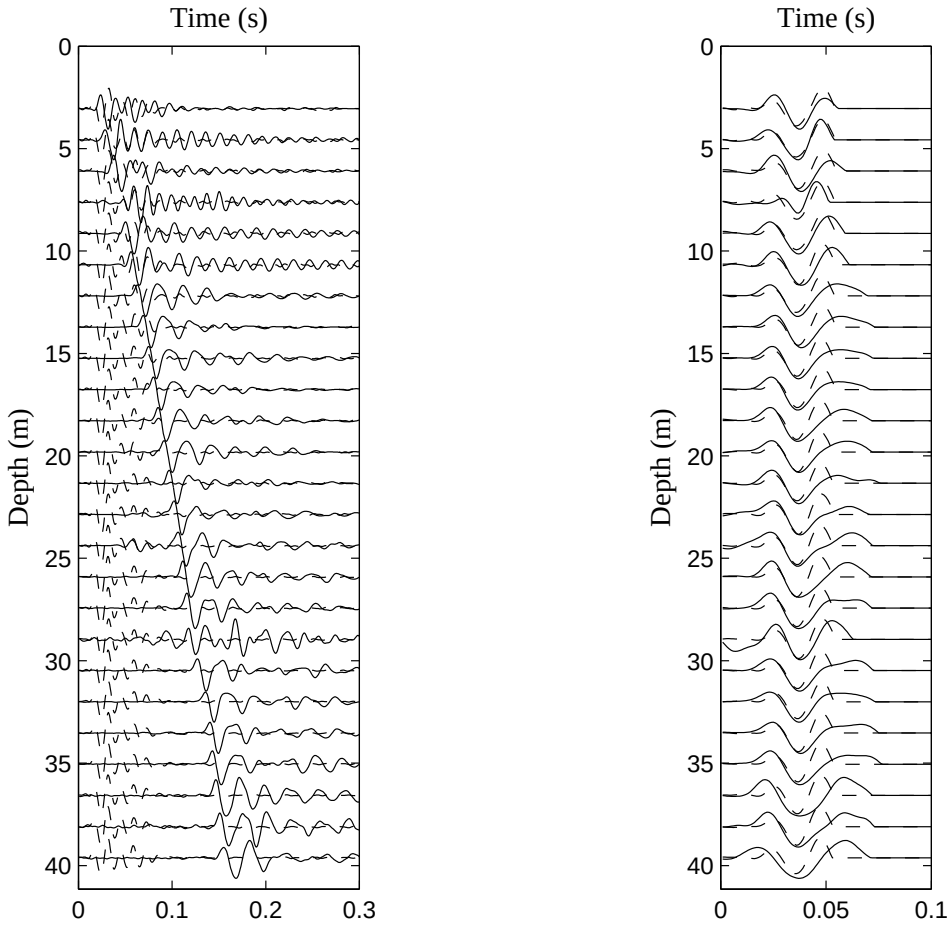

Figure 5: LEFT: Data recorded in the Covington borehole using a 4.5 Hz geophone (solid lines) and corresponding surface monitor traces (dashed lines). RIGHT: first cycles of the traces on the left used for the attenuation analysis.

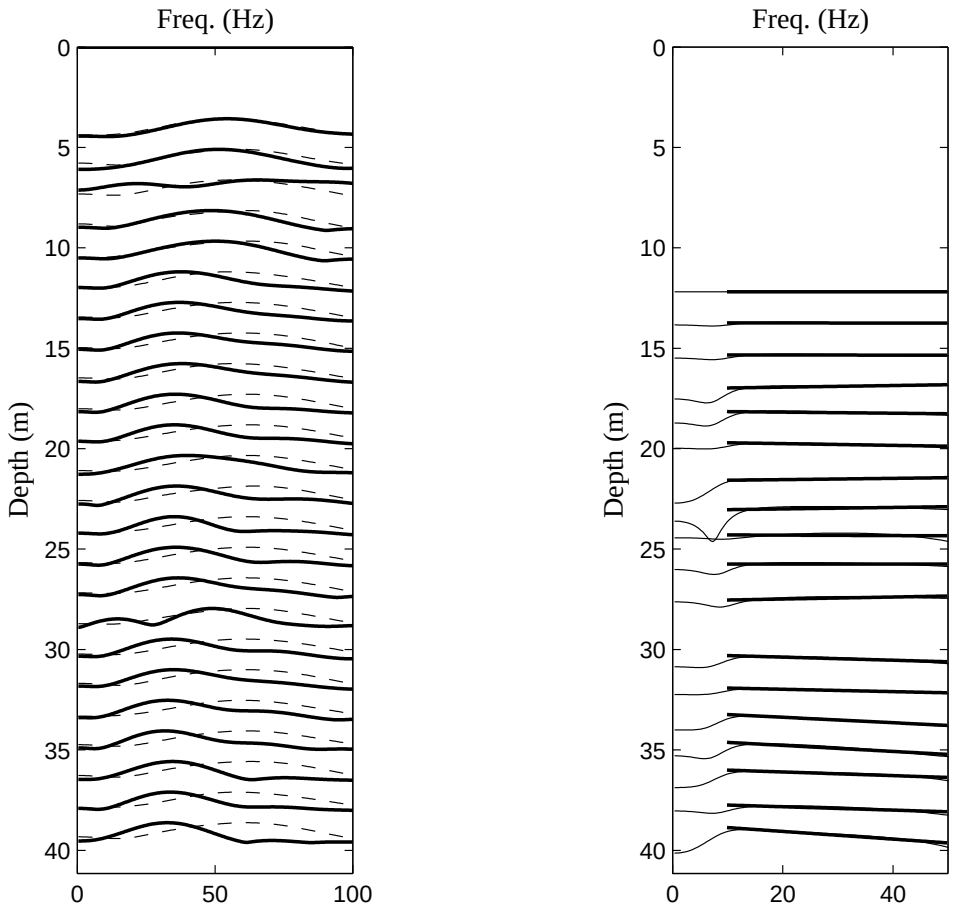

Figure 6: LEFT: Normalized spectra for the data on the right of Fig. 5. RIGHT: Spectral ratios for selected depths using the spectrum for the shallowest trace as reference (note that the ratio is a straight line). The bold line is the least-squares best fit line used to compute $\alpha(z)$ (see eqn. (3)).

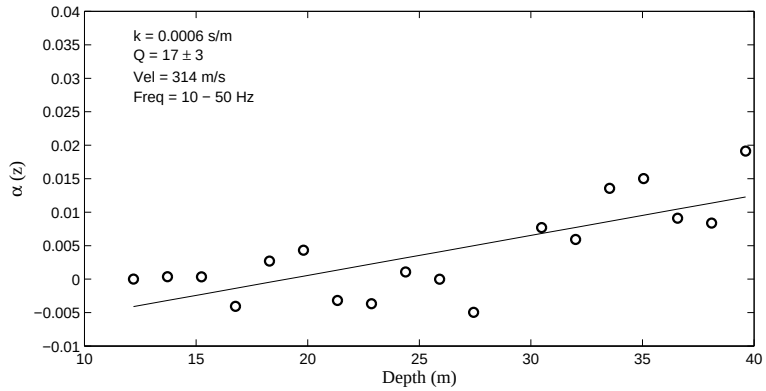

Figure 7: Attenuation curve for the Covington data for the 4.5 Hz geophone. Circles represent the cumulative attenuation α derived from Fig. 6. The best-fit line is also shown.

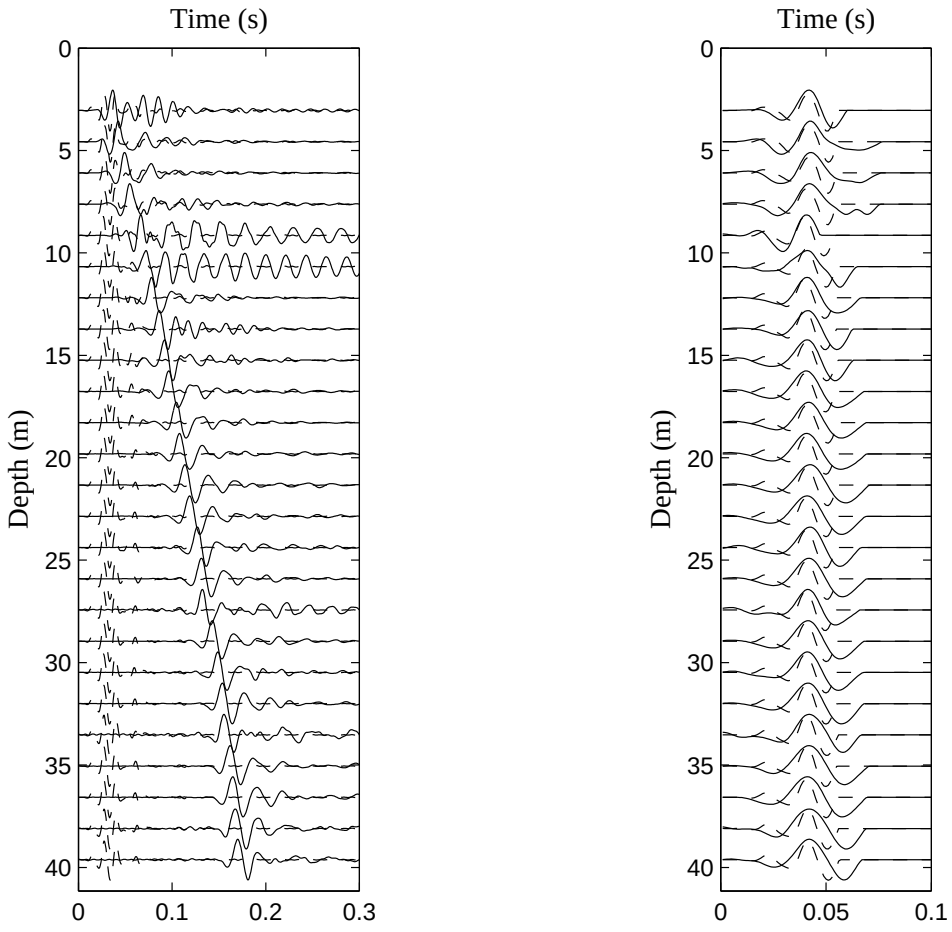

Figure 8: LEFT: Data recorded in the Shelby Farms borehole using a 10 Hz geophone (solid lines) and corresponding surface monitor traces (dashed lines). RIGHT: first cycles of the traces on the left used for the attenuation analysis.

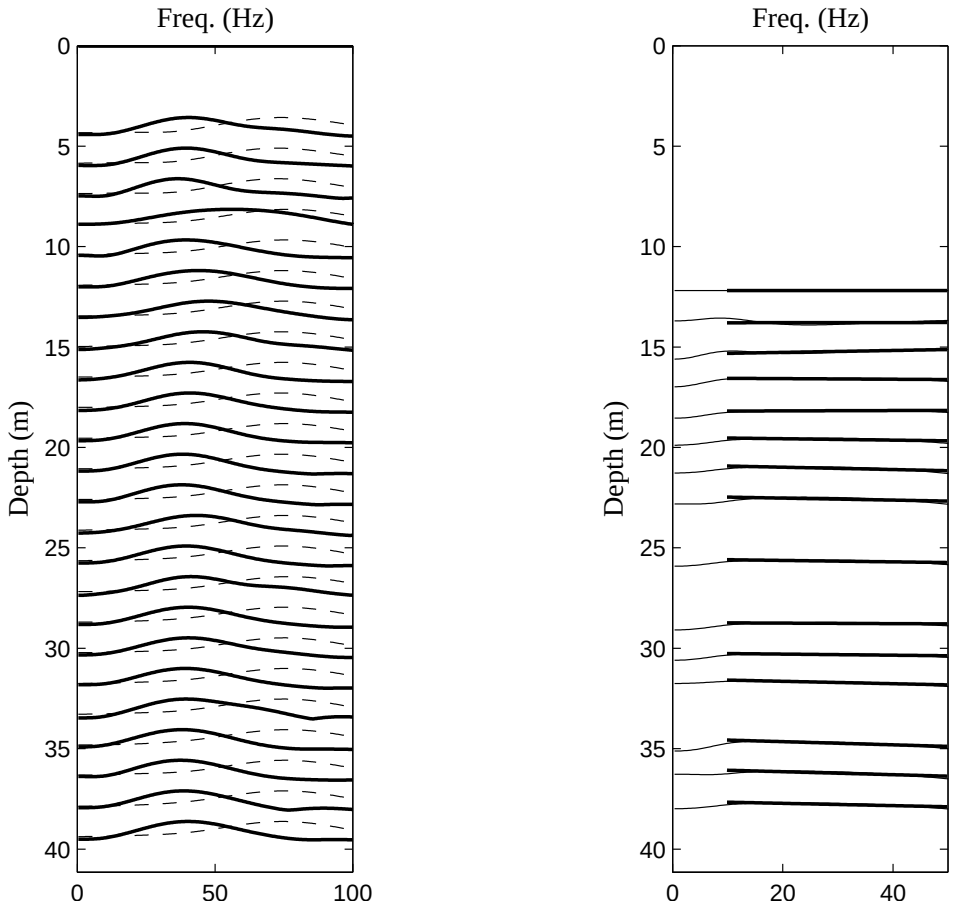

Figure 9: LEFT: Normalized spectra for the data on the right of Fig. 8. RIGHT: Spectral ratios for selected depths using the spectrum for the shallowest trace as reference (note that the ratio is a straight line). The bold line is the least-squares best fit line used to compute $\alpha(z)$ (see eqn. (3)).

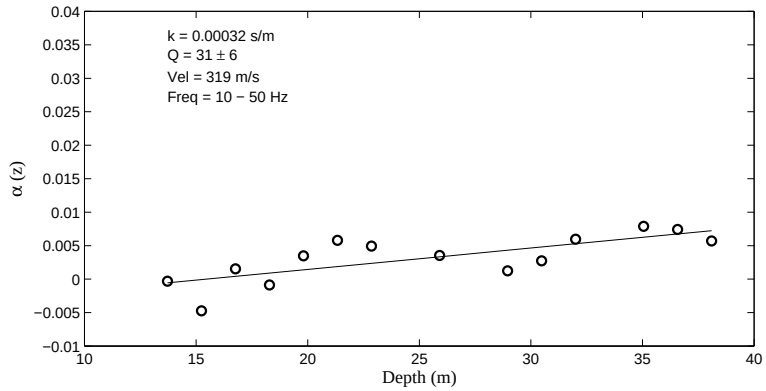

Figure 10: Attenuation curve for the Shelby Farms data for the 10 Hz geophone. Circles represent the cumulative attenuation α derived from Fig. 9. The best-fit line is also shown.

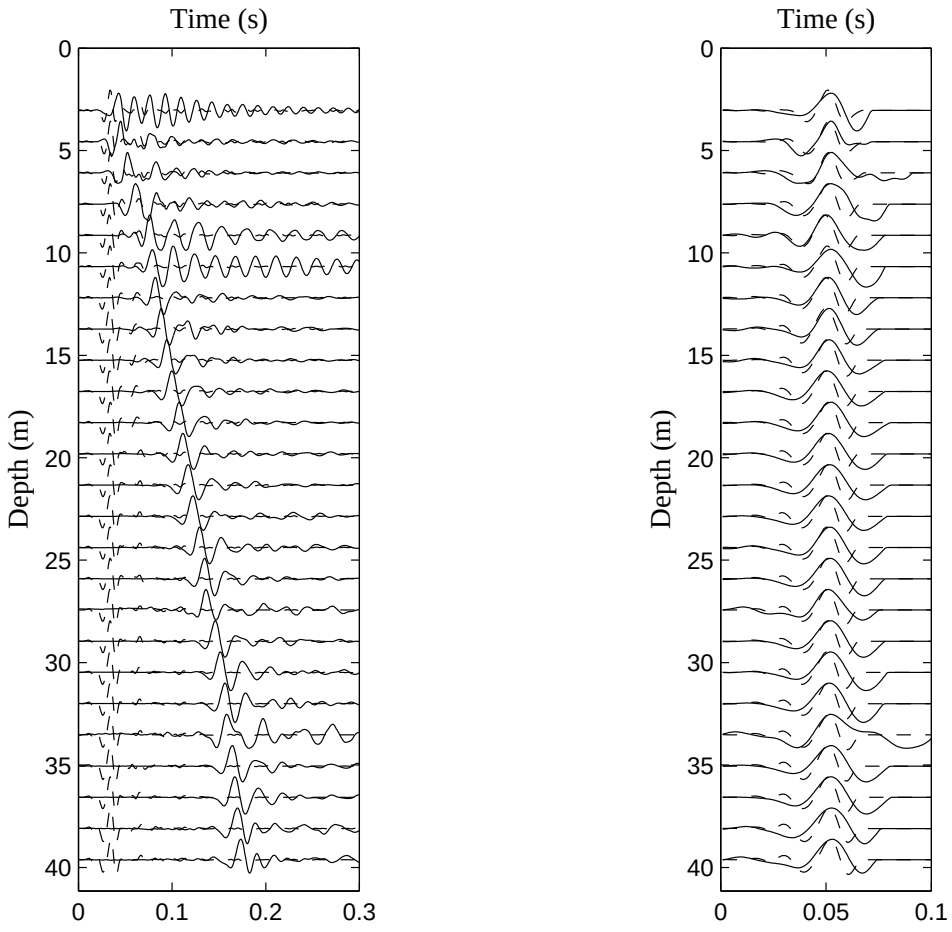

Figure 11: LEFT: Data recorded in the Shelby Farms borehole using a 4.5 Hz geophone (solid lines) and corresponding surface monitor traces (dashed lines). RIGHT: first cycles of the traces on the left used for the attenuation analysis.

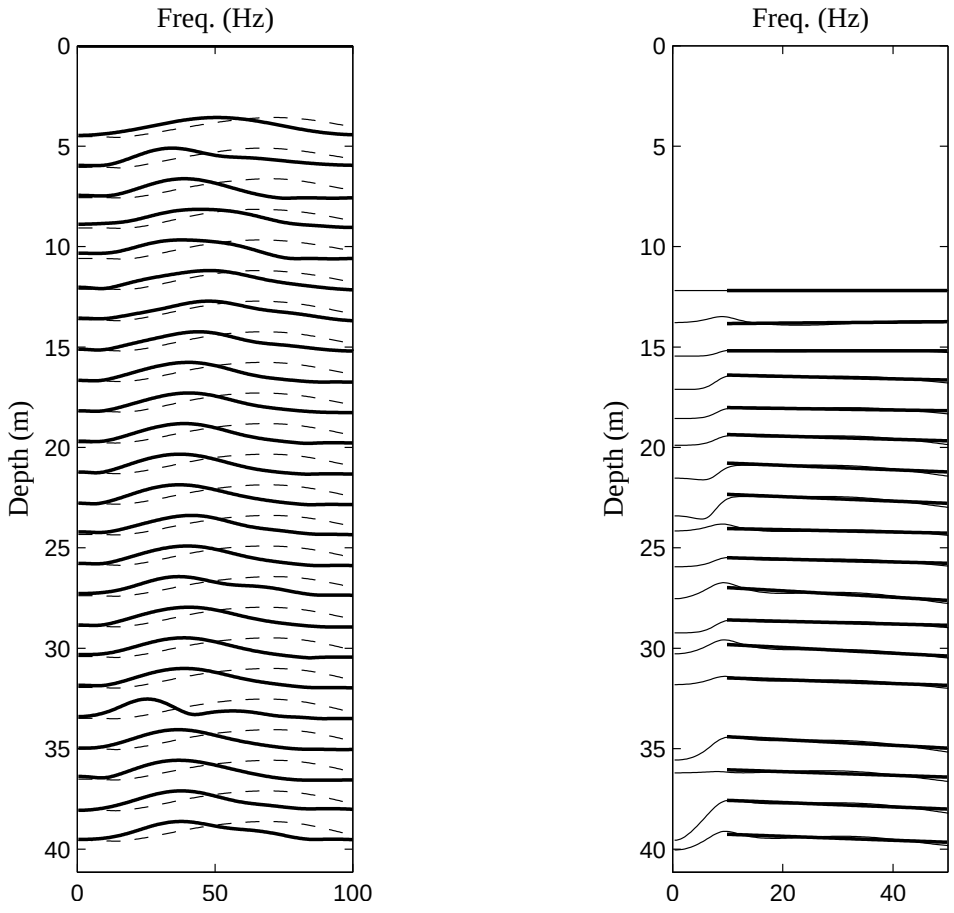

Figure 12: LEFT: Normalized spectra for the data on the right of Fig. 11. RIGHT: Spectral ratios for selected depths using the spectrum for the shallowest trace as reference (note that the ratio is a straight line). The bold line is the least-squares best fit line used to compute $\alpha(z)$ (see eqn. (3)).

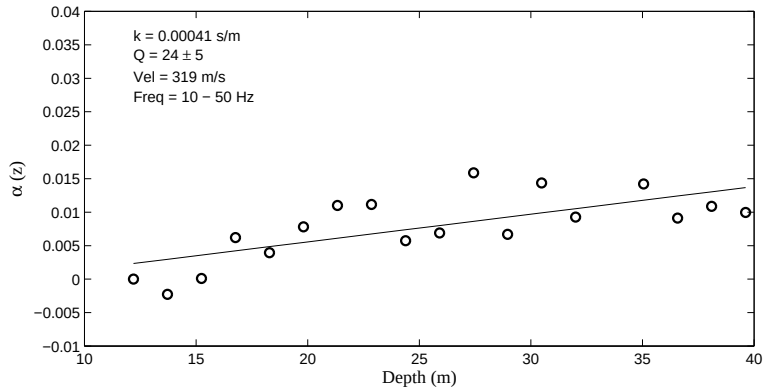

Figure 13: Attenuation curve for the Shelby Farms data for the 4.5 Hz geophone. Circles represent the cumulative attenuation α derived from Fig. 12. The best-fit line is also shown.

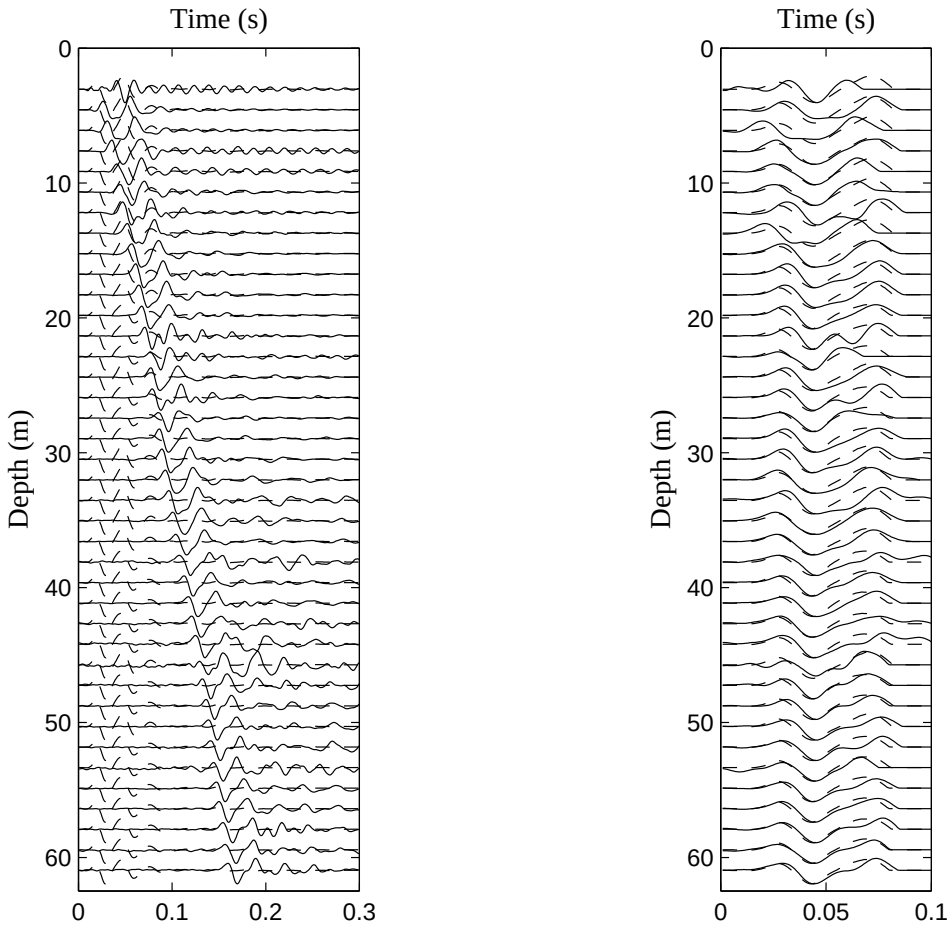

Figure 14: LEFT: Data recorded in the Brownsville borehole using a 10 Hz geophone (solid lines) and corresponding surface monitor traces (dashed lines). RIGHT: first cycles of the traces on the left used for the attenuation analysis.

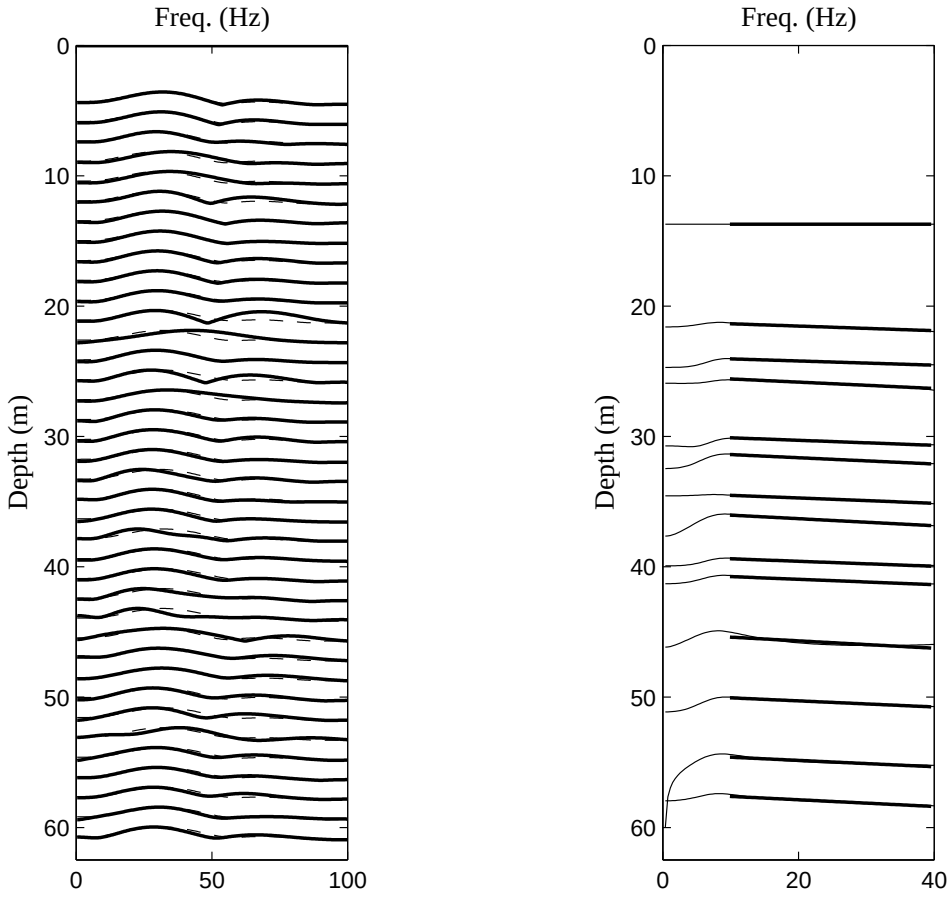

Figure 15: LEFT: Normalized spectra for the data on the right of Fig. 14. RIGHT: Spectral ratios for selected depths using the spectrum for the shallowest trace as reference (note that the ratio is a straight line). The bold line is the least-squares best fit line used to compute $\alpha(z)$ (see eqn. (3)).

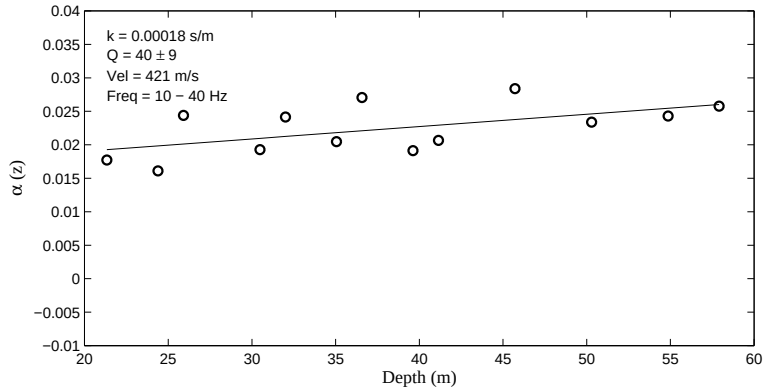

Figure 16: Attenuation curve for the Brownsville data for the 10 Hz geophone. Circles represent the cumulative attenuation α derived from Fig. 15. The best-fit line is also shown.

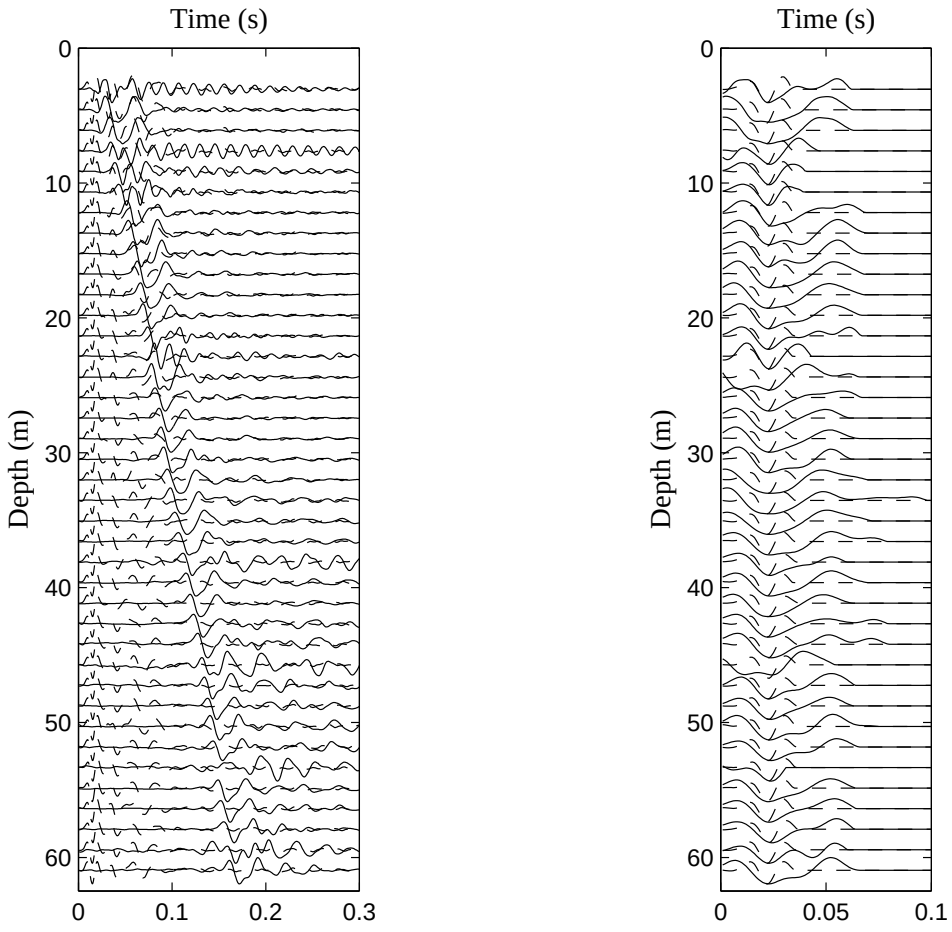

Figure 17: LEFT: Data recorded in the Brownsville borehole using a 4.5 Hz geophone (solid lines) and corresponding surface monitor traces (dashed lines). RIGHT: first cycles of the traces on the left used for the attenuation analysis.

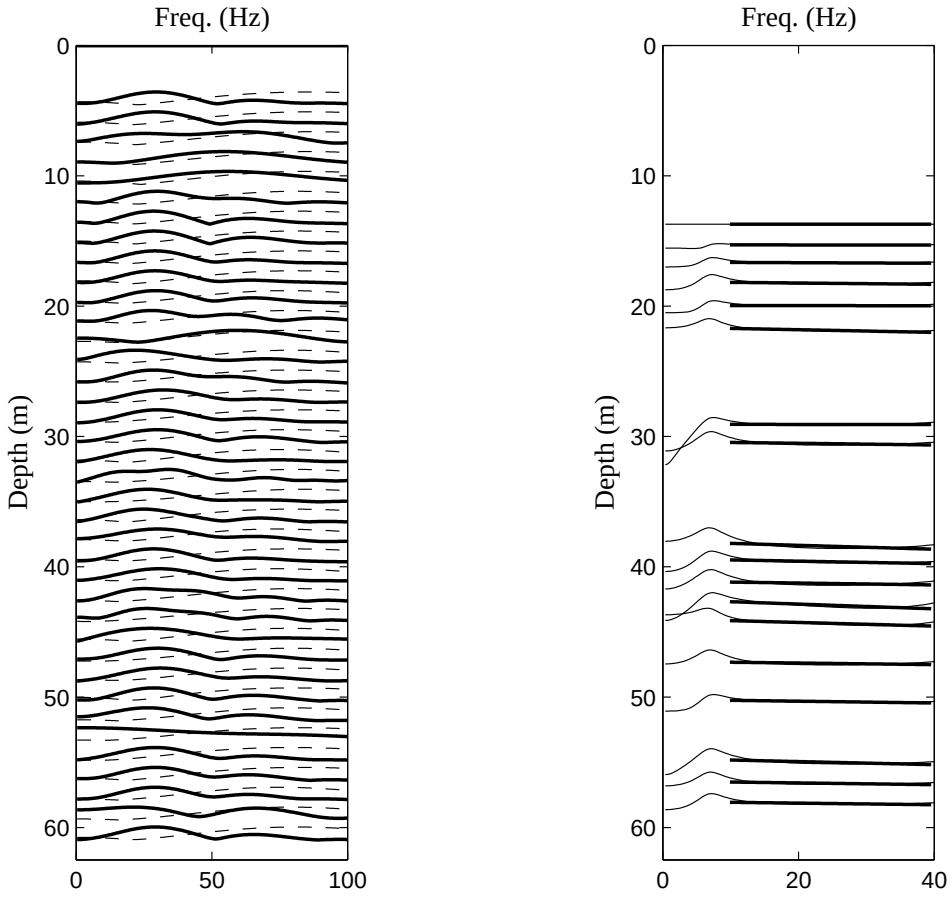

Figure 18: LEFT: Normalized spectra for the data on the right of Fig. 17. RIGHT: Spectral ratios for selected depths using the spectrum for the shallowest trace as reference (note that the ratio is a straight line). The bold line is the least-squares best fit line used to compute $\alpha(z)$ (see eqn. (3)).

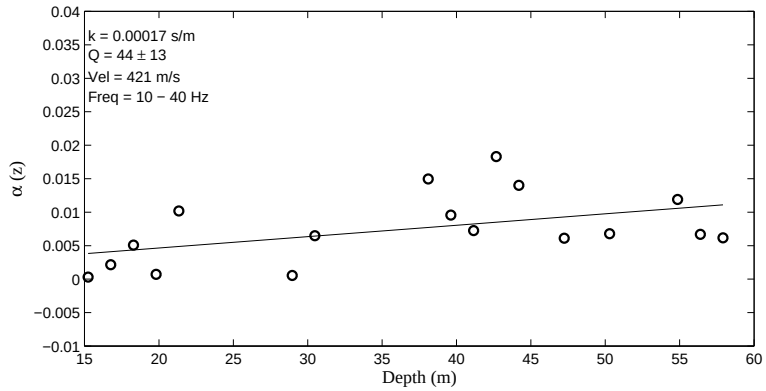

Figure 19: Attenuation curve for the Brownsville data. Circles represent the cumulative attenuation α derived from Fig. 18. The best-fit line is also shown.

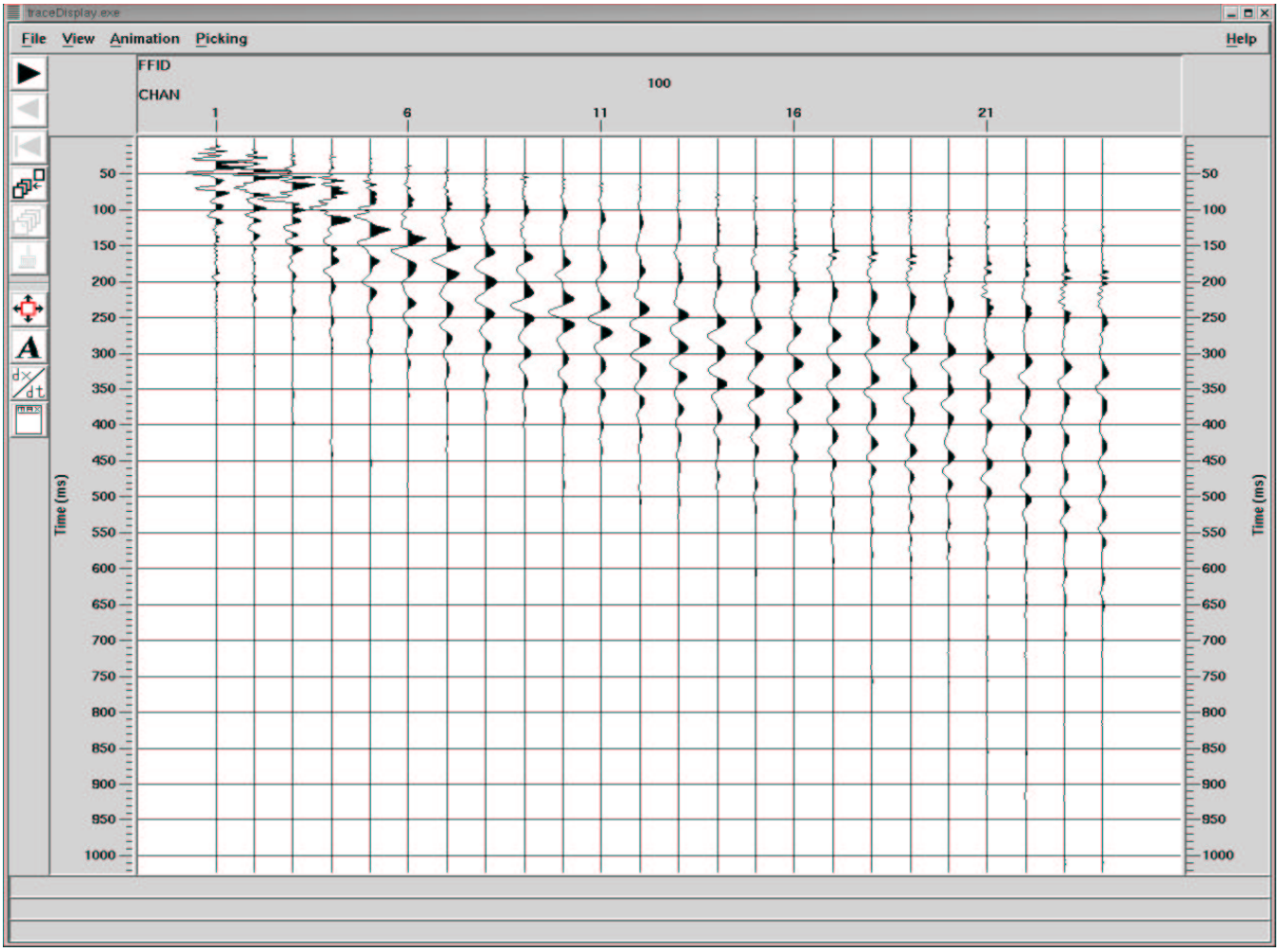

Figure 20: *SH* wave refraction data collected next to, and centered at the Brownsville borehole. The receiver separation is 1.8 m. The source was a sledgehammer impacting on an I-beam located 1.8 m from the first geophone (channel 1).

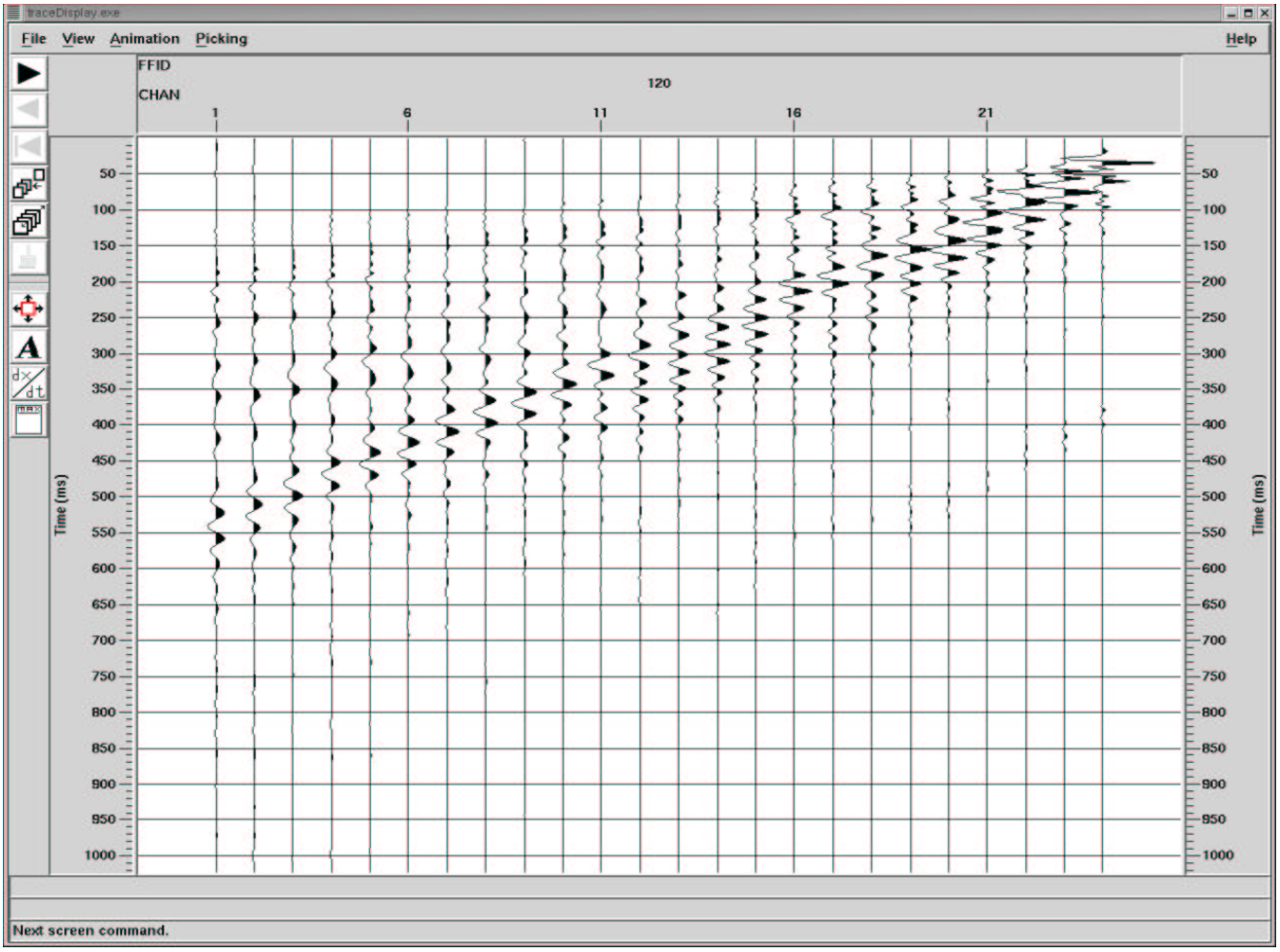

Figure 21: *SH* wave refraction data collected next to, and centered at the Brownsville borehole. The receiver separation is 1.8 m. The source was a sledgehammer impacting on an I-beam located 1.8 m from the last geophone (channel 24).

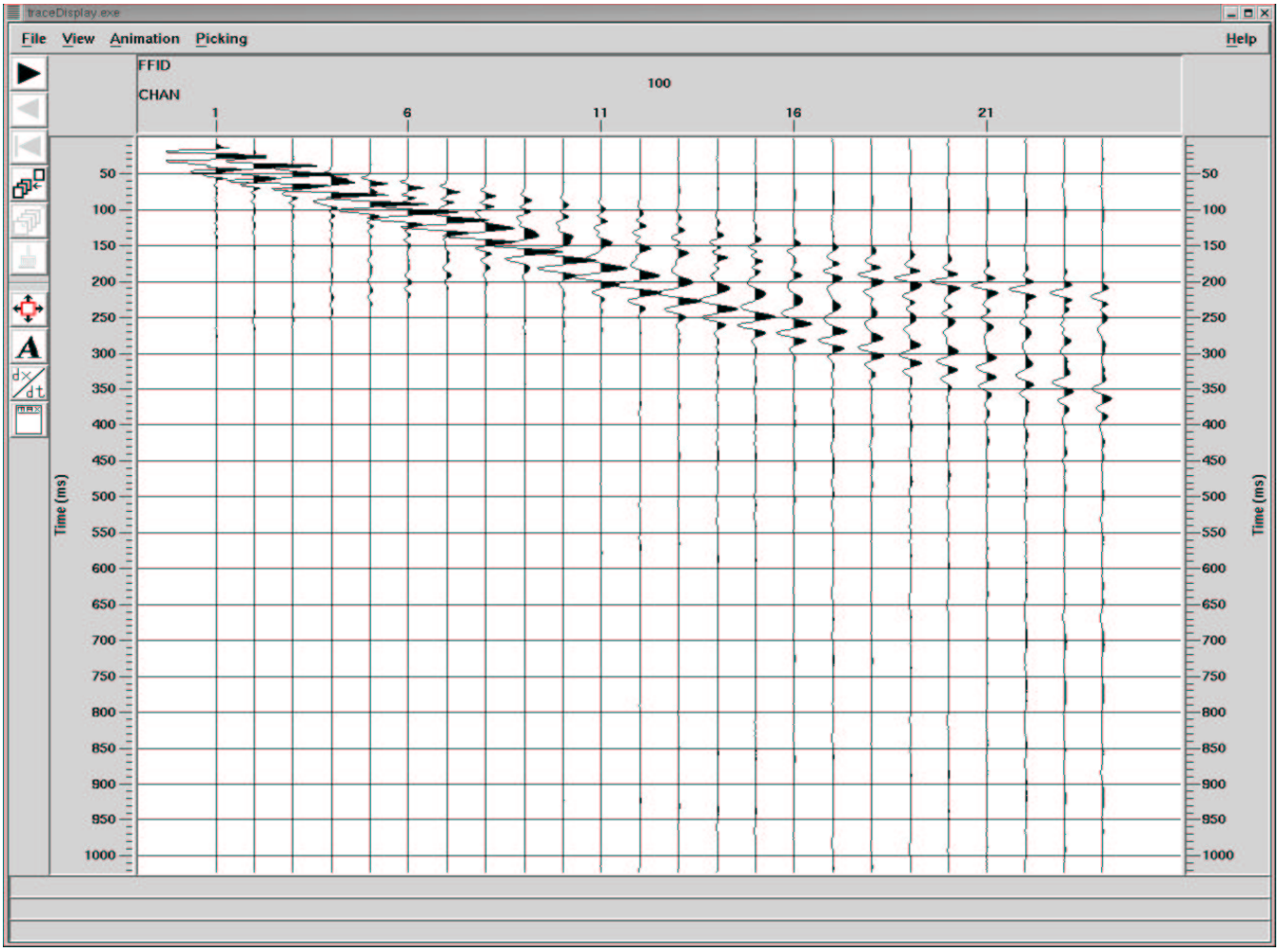

Figure 22: *SH* wave refraction data collected next to, and centered at the Jackson borehole. The receiver separation is 1.8 m. The source was a sledgehammer impacting on an I-beam located 1.8 m from the first geophone (channel 1).

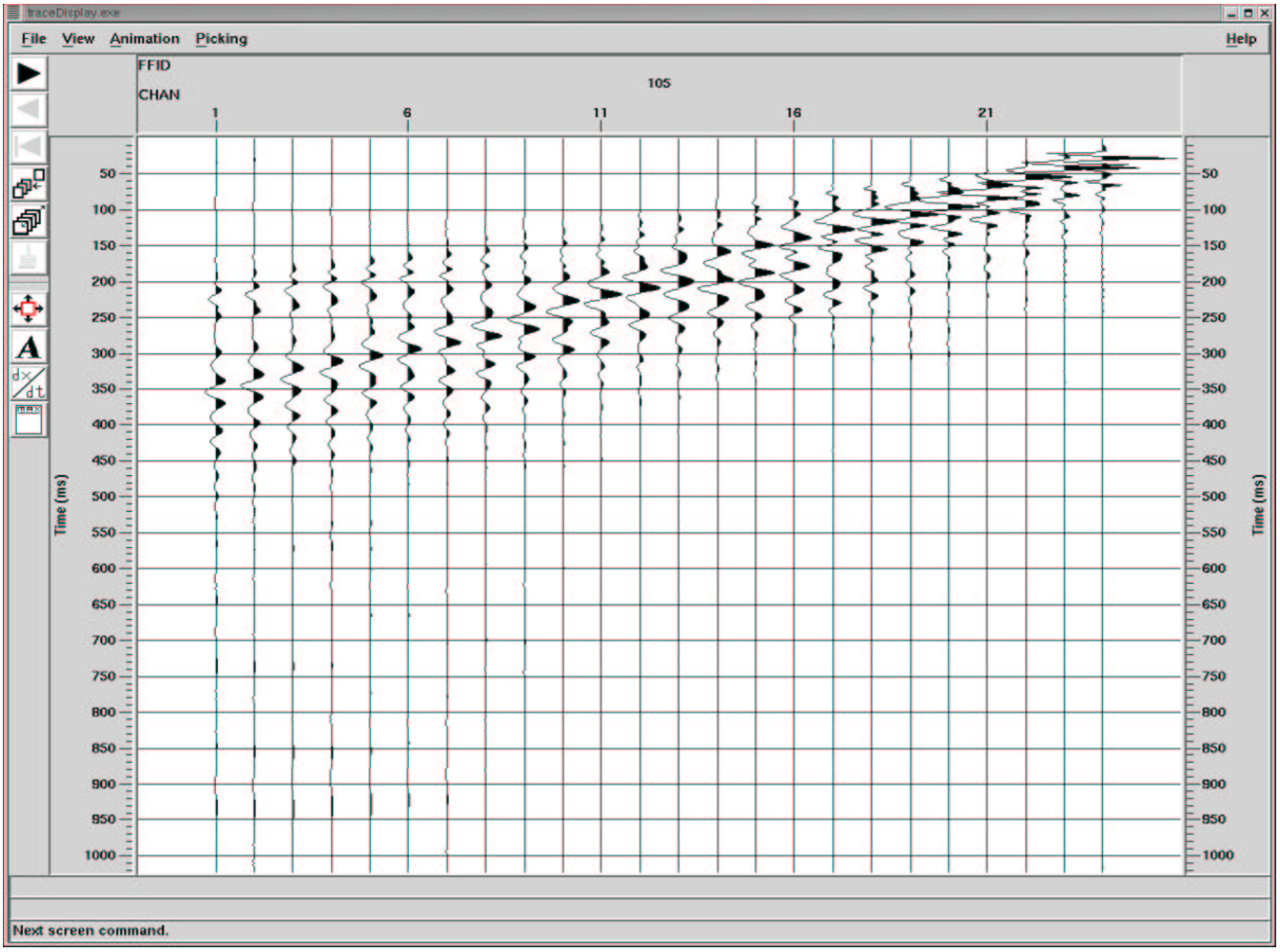

Figure 23: *SH* wave refraction data collected next to, and centered at the Jackson borehole. The receiver separation is 1.8 m. The source was a sledgehammer impacting on an I-beam located 1.8 m from the last geophone (channel 24).